



Effect of major factors on broadband natural frequency energy harvesting for rectangular and L- shaped cantilever harvesters

Sallam A. Kouritem¹ · Hassan A. El-Gamal¹ · Khaled T. Mohamed¹

Received: 9 May 2022 / Accepted: 16 March 2023 / Published online: 29 March 2023
© The Author(s) 2023

Abstract

A small amount of natural frequency deviation extremely decreases the output power. So, a multi-mass single harvester (bending harvester) was utilized to enlarge the bandwidth of the natural frequency. We constructed three models to study the effect of increasing the concentrated masses on increasing the bandwidth natural frequency. We used Finite Element Metho (FEM (COMSOL to model and simulate the three models. Moreover, we constructed an L-shaped harvester with concentrated masses to compare the rectangular harvester with concentrated masses. The results prove that increasing the number of concentrated masses increases the output power and broadband natural frequency. Moreover, the results indicate that the harvester cantilever with concentrated masses gives more output power and broadband than the L- shaped harvester for the same volume. Also, our research studied the harvester parameter effects on the output power. This study found that the increase in beam length and mass height increases the output power while the increase in piezoelectric thickness and damping ratio decreases the output power and bandwidth frequency. We validated our proposed model through a comparison with others' preceding experimental results and it showed a good agreement. The harvester with a high width/length ratio gives a larger wideband natural frequency.

1 Introduction

Researchers, in the energy harvesting field, are getting more interested in vibration energy harvesting due to its significant effect on harvested energy. The harvested energy can be utilized in structural health observing applications to provide the wireless sensors, actuators, and small electronic instruments with the required power. Our aim in this work is to broaden the operating natural frequency and maximize the harvested power. If we can broaden the natural frequency to maximize the power, the batteries may be substituted. Also, the maintenance time and effort can be reduced. In 1995 Williams and Yates (Williams and Yates 1995) discovered the energy

harvesting of vibration, designed and modified (Williams and Yates 1996) a base excitation model that presents electrical output power from energy harvesting.

Much research, in the field of natural frequency broadening, was devoted to enlarging the frequency range and increasing the efficiency of the harvester. For example, Liu et al. (Andrzej and Krzysztof 2016) established a stopper for a high natural frequency cantilever to harvest the energy. This stopper can convert the external random vibration to a self-vibration. The advantages of this harvester were to broaden the frequency range and increase the harvested power. Also, Huicong et al. (Lumentut and Howard 2013) created an experimental and analytical broadband frequency study. Their harvester was a cantilever with two side stoppers. Also, the parameters such as the base excitation acceleration, damping ratio, frequency features, and stopper distance were included. Liu et al. (Roundy et al. 2003) investigated the methodology to broaden the frequency using the aspects of frequency up-conversion. Chen et al. (Chen et al. 2013) used the band gap phenomena to enlarge the natural frequency band. Also, the effects of various parameters on the natural frequency band gap were investigated. Another broad band natural frequency technique is using a group of graded

✉ Sallam A. Kouritem
Sallam.kouritem@alexu.edu.eg

Hassan A. El-Gamal
ha_elgamal@yahoo.com

Khaled T. Mohamed
ktawfik64@alexu.edu.eg

¹ Department of Mechanical Engineering, Faculty of Engineering, Alexandria University, Alexandria 21544, Egypt

array harvesters to produce graded natural frequencies, thus broad band natural frequency (Yildirim et al. 2017; Song et al. 2018; Liu et al. 2008; Ferrari et al. 2008; Lien and Shu 2012). Li et al. (Lia et al. 2020) developed a broadband bending-torsion L-shaped device. Cao (Cao et al. 2019) proved that the operating frequency bandwidth can be widened by increasing the stiffness of the fundamental layer and decreasing the gap distance of the system, but the increase in operating frequency bandwidth came at the cost of reducing peak voltage. Wu and Lee (Wu and Lee 2019) presented a unique design of the folded harvester to collect ambient vibrational energy over a wide frequency bandwidth for the operation of battery-free electronic devices. Moon et al. (Moon et al. 2018) enlarged the broadband using two masses; the first was the tuned-proof mass and the second was a conventional-proof one. Ceponis et al. (Ceponis et al. 2019) designed harvesters to harvest energy from the vibrating base in two directions to broaden the natural frequency. Shin et al. (Shin et al. 2020) demonstrated an ultra-wide bandwidth harvester with the automatic resonance tuning (ART) phenomenon. They employed this ART to adjust the harvester's natural frequency to tune the ambient vibration without the need for an external source. Khazaei et al. (Khazaei et al. 2020) presented a creative concept using geometry and material lay-up of piezoelectric energy harvesters to enhance the output power and widen the frequency. Liu et al. (Liu et al. 2012) developed an s-shape piezoelectric cantilever, with a very low and broad natural frequency, to be used with energy sources of frequencies under 30 Hz. Liu et al. (Liu et al. 2011) described the design of a microfabrication harvester and its measurements to harvest the energy of low-frequency vibration applications.

Recently, excessive research was introduced in the field of piezoelectric energy harvesting. Lafarge et al. (Lafarge et al. 2018) utilized the Bond-Graph approach to validate the simulation of the piezoelectric cantilever beams that were used to harvest a vehicle suspension vibration. Ramírez et al. (Ramírez et al. 2018) investigated an energy harvester to operate in a very low-frequency bandwidth (3–10 Hz). Hong et al. (Hong et al. 2018) studied the influence of the neutral plane on the generated power of the piezoelectric harvester. Song et al. (Song et al. 2017a) optimized the Polyvinylidene Fluoride (PVDF)-based cantilever with harvester geometry adjustment to control the stresses. Iannacci (Iannacci 2017) presented a review of the area of energy harvesting—Microelectromechanical Systems (MEMS), with a specific concentration on vibration energy harvesting, especially, the piezoelectric harvester that is utilized in vibration energy sources. Mohamed et al. (Mohamed et al. 2021) utilized the COMSOL optimization module (BOBYQA solver) and the genetic algorithm to optimize the shape of the energy-

harvesting piezoelectric cantilever to maximize the output power. Kouritem et al. (Kouritem et al. 2022) introduced a broadband technique using the tuning of passive masses on an array of the piezoelectric energy harvester. The introduced solution can manage the lowering of the power between the peaks. Bani-Hani et al. (Bani-Hani et al. 2022) designed a sensor of 17 harvesters to sense the vibrations resulting from an Earthquake excited in the frequency range (1–17 Hz). Kouritem et al. (Kouritem et al. 2022b; Kouritem and Altabay 2022; Altabay and Kouritem 2022) utilized the Automatic Resonance Technique for a cantilever of piezoelectric to produce wideband natural frequency. Erturk and Inman (Erturk and Inman 2009) investigated experimentally and analytically a bimorph with different connections (series and parallel). Kouritem (Kouritem 2021) showed and studied the output power of the first and second-mode shapes. Bani-Hani et al. (Bani-Hani et al. 2023) proposed a Genetic Algorithm optimization technique to harvest power of Impact Force that be utilized as a sensing device, Analytical and Finite Element Investigation Naqvi et al. (Naqvi et al. 2022; Shaukat et al. 2023) presented a complete review of some vibration sources. Some parameters are optimized in this paper using the iterative optimization technique (Kouritem and Elshabasy 2021; Elshabasy and Kouritem 2020; Kouritem et al. 2022c).

The importance of natural frequency widens, is that the tuning of a piezoelectric energy harvester to a specific resonance frequency may not be an effective methodology, since most of the energy sources have a wide operating natural frequency and a small amount of variation in the excitation frequency results in a great drop in the output power. The wide (broad) band is defined by increasing the operating or resonance frequency that produces maximum power. The common disadvantage in the earlier broadband natural frequency schemes is the need for extra devices. Extra devices required, besides the harvester, like the stopper or an external magnet is essential to broaden natural frequency. Besides, the rough matching and tuning between the excitation band's natural frequency and the harvester. The drawbacks and limitations of previous studies (see Table 1) motivate us to propose our broadband natural frequency harvester, a single harvester without extra devices can be utilized to widen the natural frequency. Also, the sliding masses can be employed to change the operating broad band natural frequency. The first aim of this paper is to study the effect of the multi-mass harvester on broadband to be employed in the low natural frequency applications where many vibration sources produce a low frequency of less than 100 Hz (Roundy et al. 2003). The low natural frequencies of these sources need to broaden to highly increase the system efficiency. The second aim is to study the effect of

Table 1 Review, limitations and drawbacks of literature broadband natural frequency methods

Reference	Technique(s)	Limitations
Song et al. (2018)	External magnet	Massive dimensions External magnet Slight bandwidth improvement
Yildirim et al. (2017); Song et al. (2018); Liu et al. (2008); Ferrari et al. (2008); Lien and Shu (2012)	Graded array harvesters	Small output power between the resonance frequencies Large dimensions
Kouritem et al. (2022a)	Mass tuning of array of harvesters	Optimal angle may be changed for different array dimensions
Kouritem et al. (2022b); Kouritem and Altabay (2022)	Resonance tuning using the active method	Small net output power Sensor and actuator are required

harvester parameters like the damping ratio, thickness, and length on the output power and natural frequency bandwidth to reach the optimal design. Also, this research compares the effectiveness of the bending stress harvester and the torsion-bending harvester in both widens the natural frequency and increases the output power.

The remaining sections of the paper is as follows; the second part contains a Broadband Vibration. The third section describes L-Shaped cantilever with three concentrated masses. The fourth section presents the Effect of harvester parameters on the output power. Section five describes Finite Element Models validation. Finally, the conclusions are presented.

2 Broadband vibration

Broadband vibration energy harvesting using concentrated masses on a cantilever will be presented in this section. The novelty in this part is the widening of the resonant bandwidth of a piezoelectric harvester based on the values and the numbers of the concentrated masses. The effect of the masses on the vibration band gap was studied through the three models, listed below, using a COMSOL finite element simulation.

The power output depends on the resistance, inertial mass, base excitation, damping coefficient, natural frequency, capacitance, and load resistance. The equation of power, utilized in COMSOL modeling for all cases in this research, is given by Lefeuvre et al. (M. Peigney et al. 2013). The output power equation as a function in base excitation and inertial mass is expressed as:

$$Power = \left(\frac{R\alpha_2^2}{\left(\frac{\pi}{2} + Rc_p\omega_n\right)^2} \frac{\omega_n^4 U^2 M^2}{\left(C_v + \left(2R\alpha_2^2 / \left(Rc_p\omega_n + \left(\frac{\pi}{2}\right)^2\right)\right)\right)^2} \right) \quad (1)$$

After the reduction of the output power can be expressed as:

$$Power = V_{re} \left(\frac{2\alpha_2}{\frac{\pi}{2} + Rc_p\omega_n} + C_v \frac{\frac{\pi}{2} + Rc_p\omega_n}{\alpha_2 R} \right) \quad (2)$$

where, α_2 represents the electromechanical coupling properties of piezoelectric materials, V_{re} is the rectified voltage (V), c_p is the capacitance (C/V), C_v is the damping coefficient (N/ms), M is the dynamic mass (Kg), U is the base excitation (m), $U\omega_n^2$ is the base excitation (m/s²), ω_n is the natural frequency (Hz), and R is the load resistance (Ω).

2.1 Cantilever models

In this study, we will consider the following cantilever types

1. Cantilever without any concentrated masses.
2. Cantilever with three concentrated masses.
3. Cantilever with six concentrated masses.

One method to attain a relatively broadband response is to tune the number of concentrated masses. The harvester base material is copper with a density of 8960 kg/m³ and 110GPa elastic modulus. The piezoelectric material is PZT-5H with a density of 7500 kg/m³ and 62GPa elastic modulus. The masses material is steel with a density of 7850 kg/m³ and elastic 200GPa modulus. Figure 1 shows the harvester with concentrated masses. The model is excited by the acceleration of 6 m/s² equal to the acceleration of a vibrating bridge (Lefeuvre et al. 2007).

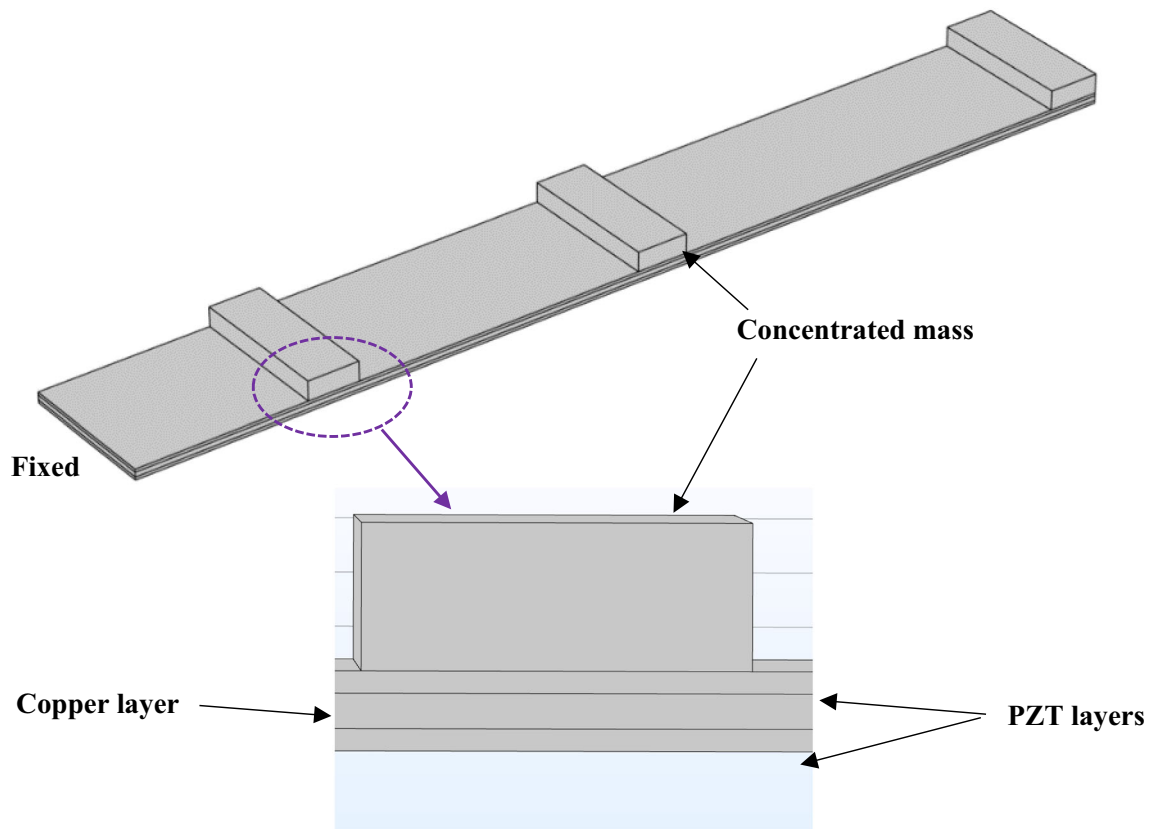


Fig. 1 The harvester with concentrated mass configuration

2.2 The natural frequency study of the harvesters

To determine the natural frequencies, we created an Eigen-frequency study. Table 2 reveals the material properties and values of harvester parameters utilized in this study (Mehrabi et al. 2020). The dimensions of mass (length \times width \times height) of three masses model are $3.5 \times 9.92 \times 1.35$ mm which is equal to 0.36 g/each mass. The dimensions of mass (length \times width \times height) of six masses model are $3.5 \times 9.92 \times 0.675$ mm which equals 0.18 g/each mass. The dimensions of the three models are the same (see Table 2). Table 3 shows the mesh convergence study of the natural frequency. The study is utilized to reach maximum mesh accuracy. Tetrahedra is

Table 3 Mesh convergence study based on natural frequency

Number of elements	7000	15,500	46,977	50,000
Mode 1 frequency (Hz)	68.82	68.73	68.66	68.66
Mode 2 frequency (Hz)	431.14	430.34	429.89	429.28

employed as mesh element type to enhance the mesh quality. The natural frequencies of the three models are listed in Table 4, while their deflections are summarized in Table 5. The results in Table 4 are at acceleration 0.6 g. The dimensions of the models are shown in Figs. 2, 3, and 4. Figure 2 shows the first five natural frequencies and

Table 2 Material properties and values of harvester parameters utilized in this study (Mehrabi et al. 2020)

Parameters	Copper	PZT-5H	Material	Copper	Piezoelectric
Length (mm)	69.9	69.9	Density (kg m^{-3})	8960	7500
Width (mm)	9.92	9.92	Young's modulus (GPa)	110	62
Thickness (mm)	0.31	0.2	Poisson's ratio	0.33	0.31
			Piezoelectric constant d_{31} (pm/v)	–	– 274
			Permittivity constant(nF/m)	–	3130

Table 4 The natural frequencies of the first five mode shapes (Hz)

	Mode1	Mode2	Mode3	Mode4	Mode5
Harvester without added mass	68.66	429.89	930.5	1074.1	1204.6
Harvester with three masses	62.703	378.57	909	989.14	1083.2
Harvester with six masses	64.113	418.49	925.1	1070.4	1189.8

Table 5 The deflection of the first five mode shapes (mm)

	Mode1	Mode2	Mode3	Mode4	Mode5
Harvester without added mass	2	0.35	0.6	0.8	0.12
Harvester with three masses	1.8	0.25	0.6	0.35	0.09
Harvester with six masses	1.7	0.25	0.6	0.25	0.08

mode shapes of a harvester without masses (simple model). This model was utilized to reveal the effect of the concentrated masses. Figure 3 shows the first five natural frequencies and mode shapes of a harvester with three masses, while Fig. 4 shows the first five natural frequencies and mode shapes of a harvester with six masses.

2.3 The simulation results of the broad-band harvesters

In this section, the simulation results of the three harvesters are presented, summarized, and compared to show the importance of the concentrated masses in increasing the power output and broadband frequency. All harvesters were subjected to the same base excitation (6 m/s^2 , same volume, and same inertia force).

Figure 5 shows the power output and broadband of the three harvesters. The results, summarized in Fig. 5, revealed that increasing the concentrated masses increases the broadband and power output. The broadband frequency that was determined at 5 mW of the six masses harvester, the three masses harvester, and the harvester without added mass was 7.5 Hz, 6.8 Hz, and 4.5 Hz, respectively. The increase of the broadband frequency of the six masses harvester and the three masses harvester are about 66 and 51% from the broadband frequency of the harvester without added mass, respectively. Table 6 shows that the increase of the power output per unit volume of the six masses harvester is about 12%, while for the three masses harvester is about 2.2% compared with that the harvester without added mass.

Figures 6, 7, and 8 show the two mode shapes power output of harvesters without added masses, with three masses, and with six masses respectively. The results presented by these figures prove that the second mode’s power is less than 11% of the first mode’s power and the last three modes’ power is less than 2% of it. Figure 9

shows the first mode strain of the six masses harvester. The figure highlights the location of piezoelectric materials with maximum power. Also, it indicates that the maximum stress results in the maximum strain at the fixed end.

2.4 Performance of the proposed design

The results of the earlier studies are compared to the results of the recent study. Table 7 shows that the KIM (Kim et al. 2005) reported that the power output per unit volume was $34 \times 10^{-3} \text{ mW/mm}^3$. In this study, the power per unit volume is $56.3 \times 10^{-3} \text{ mW/mm}^3$ with a 65% improvement in power per unit volume.

3 L-Shaped cantilever with three concentrated masses

The L-shaped harvester is composed of two beams, one in the x-direction and the other in the y-direction. Each beam has three layers, the top and bottom layers are from piezoelectric materials while the mid layer is copper. Also, there are three concentrated masses staked on the top layer to broadband the frequency. The L shape can be considered as both a torsional and linear spring due to the bending and the torsion stresses as represented in Fig. 10. The proposed L-shaped harvester with concentrated masses was selected to be compared with the rectangular harvester with concentrated masses and to study the effect of the combined stress on both the output power and the bandwidth frequency. Figure 10 shows the proposed L-shaped harvester with concentrated masses. Also, it reveals the first five mode shapes and their deflections. The natural frequencies of the first five mode shapes were 97.587, 284.79, 916.05, 1337.5, and 1800.1 Hz respectively. Figure 11 demonstrates the dependence of output power and voltage on the resistance to determine the optimal output power.

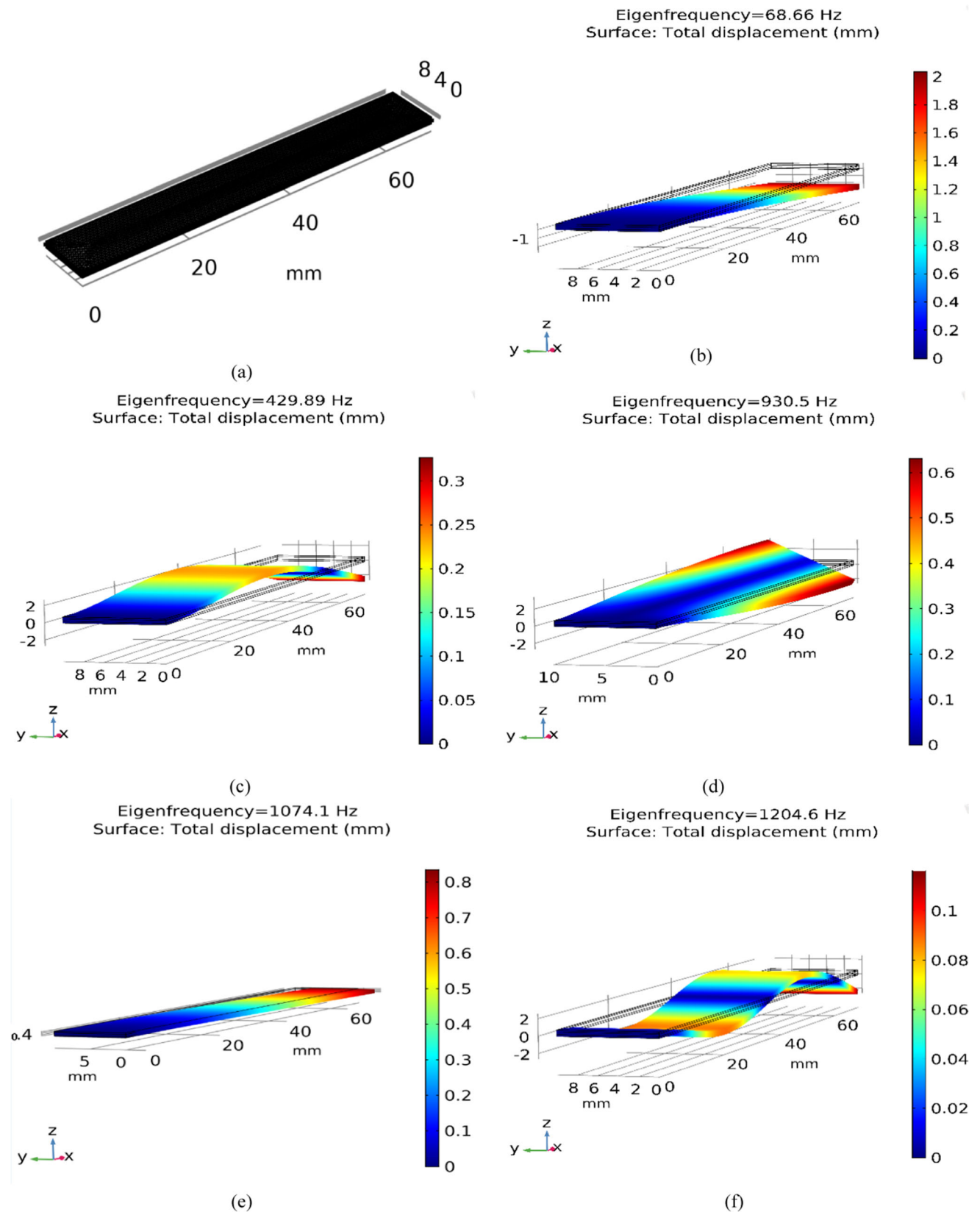


Fig. 2 The mode shapes and natural frequencies of a harvester without added masses **a** mesh model **b** first mode **c** second mode **d** third mode **e** fourth mode **f** fifth mode.

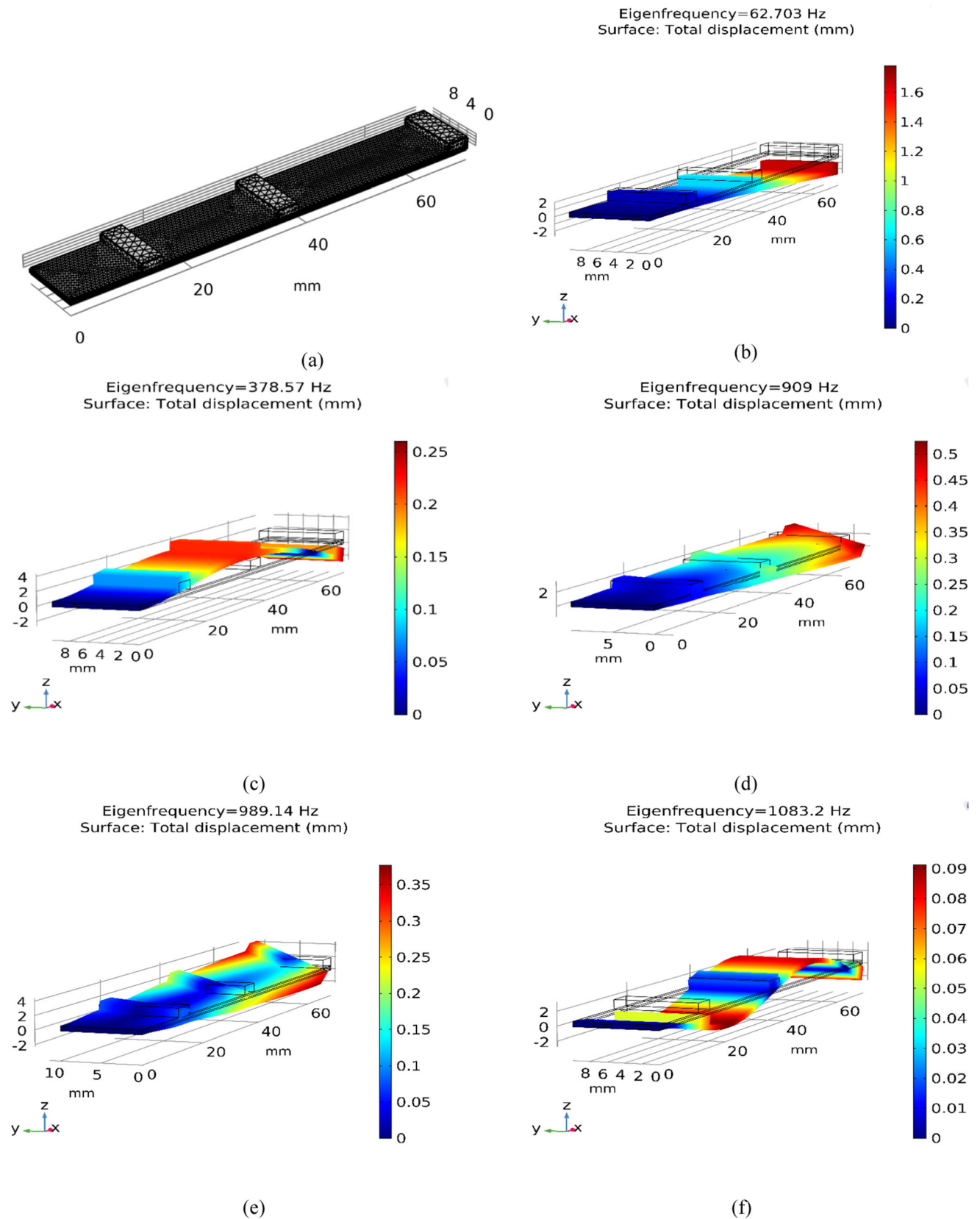


Fig. 3 The mode shapes and natural frequencies of a Harvester with three added masses **a** mesh model **b** first mode **c** second mode **d** third mode **e** fourth mode **f** fifth mode

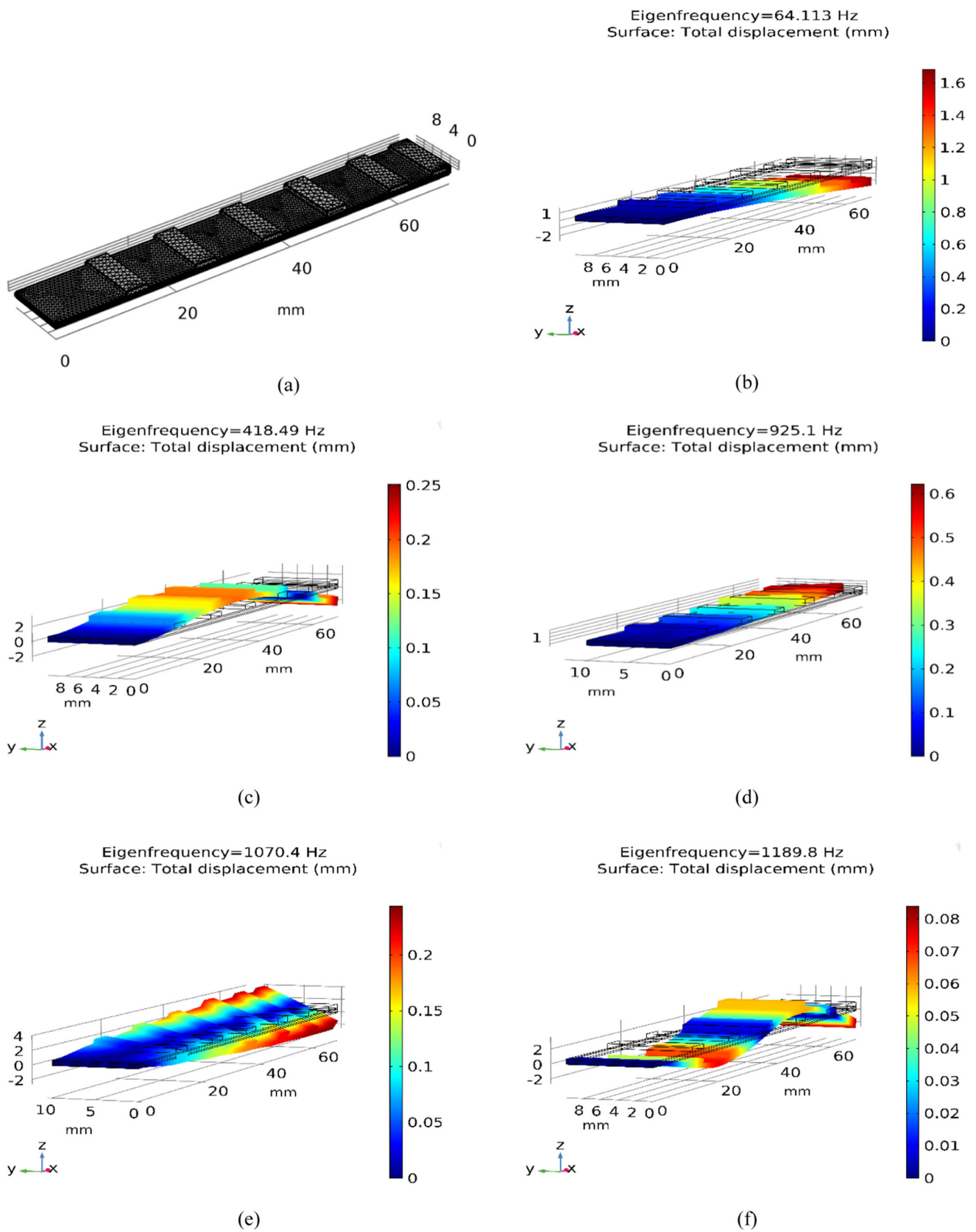


Fig. 4 The mode shapes and natural frequencies of a harvester with six added masses **a** mesh model **b** first mode **c** second mode **d** third mode **e** fourth mode **f** fifth mode

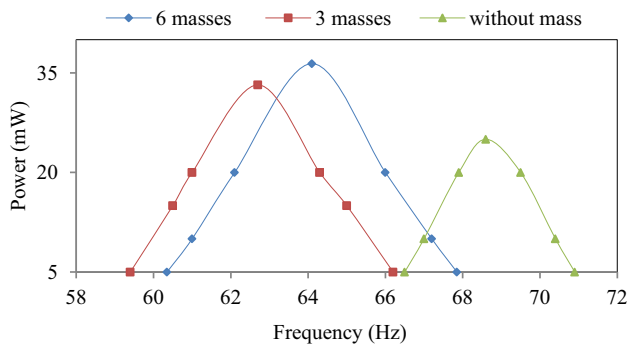


Fig. 5 The first mode and its power output of the three harvesters

Table 6 The power output of the three harvesters at 6 m/s²

	Power (mW)	Volt (V)	Volume (mm ³)	Power/volume (mW/mm ³)
Without mass	25	2.2	496.7	50.33×10^{-3}
Three masses	33.2	2.6	646.4	51.4×10^{-3}
Six masses	36.4	2.65	646.4	56.3×10^{-3}

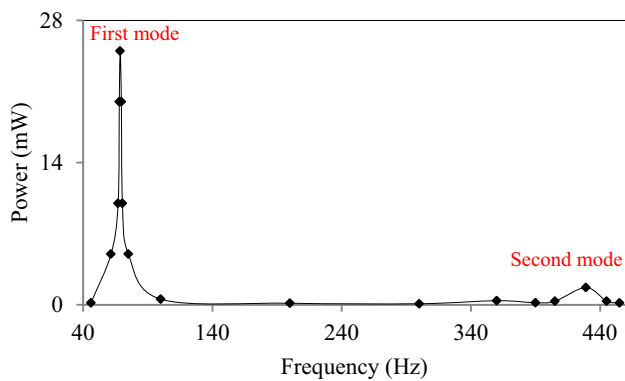


Fig. 6 The first two mode shapes and their power output for harvester without masses

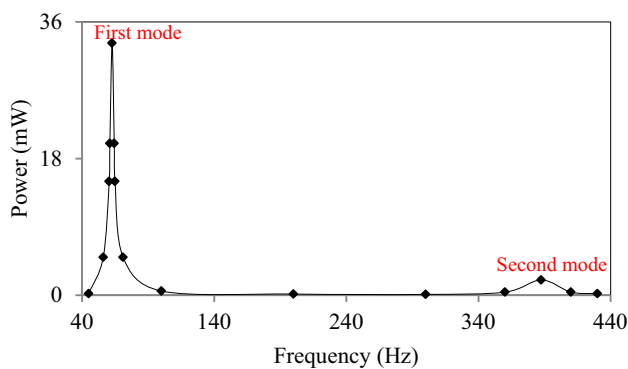


Fig. 7 The first two mode shapes and their power output for harvester with three masses

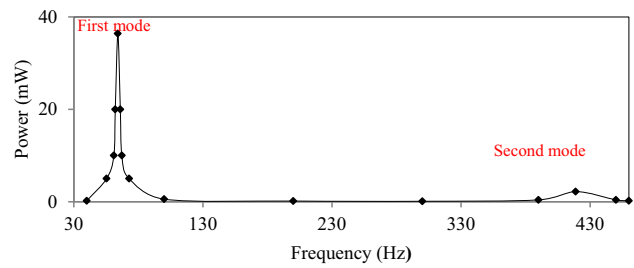


Fig. 8 The first two mode shapes and their power output for harvester with six masses

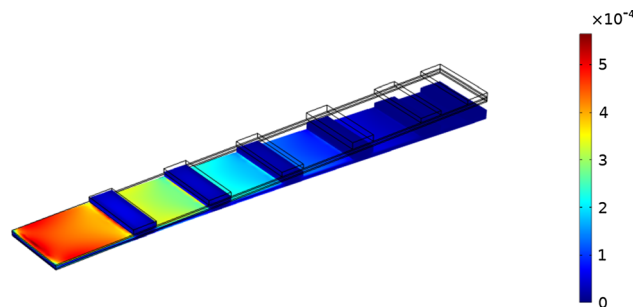


Fig. 9 The strain distribution along six masses harvester at the first mode

Figure 12 shows the output power–frequency relation. The output power was 28 mW with a harvester volume of 767.2 mm³. The power per unit volume was about 41.9×10^{-3} mW/mm³. These results prove that the L-shaped harvester, with concentrated masses, is not as effective as the rectangular harvester with concentrated masses. The low output power per unit volume of the L-shaped harvester is due to its lower bending stress compared with the high bending stress of the rectangular harvester with concentrated masses. The results of the previous section and this section indicate that the rectangular harvester cantilever with concentrated masses is more effective than the L-shaped and this effect increases with the increase of the concentrated masses number.

4 Effect of harvester parameters on the output power

In this section, a harvester with six concentrated masses is employed to study the effects of harvester parameters on the output power. Four parameters were chosen for the power optimization process: length, the thickness of the

Table 7 A comparison between the output power of earlier studies and this one

Author	Year	Piezoelectric material	Frequency (HZ)	Base excitation (g) or force	Power per volume (mW/mm ³)
Kim (Kim et al. 2005)	2005	PZT	100	70 N	34×10^{-3}
Aktakka (Failed 2011)	2011	PZT	154	1.5 g	7.6×10^{-3}
Song (Song et al. 2017b)	2015	PZT	75	3.5 g	4.27e–6
Wu (Wu et al. 2016)	2017	PZT (BiScO ₃ –PbTiO ₃)	56	0.5 g	0.804e–6
Hung (Hung et al. 2015)	2016	PZT	68	0.25 g	0.209e– 3
Present Study		PZT-5H	64.11	0.6 g	56.3×10^{-3}

mass, the thickness of the piezoelectric layer, and the damping ratio. The effects of controlling the four parameters on the output power are demonstrated in Figs. 13, 14, 15, and 16. It is observed from results in Figs. 13 and 14 that, the increase of beam length and mass height increases the bending stress and thus the output power. Figures 15 and 16 results prove that the increase in piezoelectric thickness and damping ratio decreases the output power and bandwidth frequency. Also, they indicate that the increase of the piezoelectric thickness decreases the bending stress and that the four parameters influence the output power effectively. It is not easy to evaluate the damping of the piezoelectric, which depends on mechanical loss and frequency. The natural frequency depended on the harvester dimensions, so the dimensions affect the damping of piezoelectric materials. Increasing the damping increases the resistance and decreases the vibrations, thus the generated stress and strain will be decreased, then the sensing voltage decreases. Nader et al. (Nader et al. 2004) evaluated the damping of the piezoceramics by determining the quality factor to be utilized by FEM simulations. In our investigation using FEM, a parametric study is conducted to study the effect of damping on the output power.

5 Finite element model validation

In this section we introduce a comparison between earlier studies' results and these study results, in some cases according to their availability, to validate our work. The experimental study of Erturk and Inman (Kouritem and Altabay 2022) was repeated numerically using our COMSOL model and the results were compared. The piezoelectric and substrate layers' dimensions and properties were the same as those given by reference (Kouritem and Altabay 2022) as shown in Table 7. From Table 8, it is

obvious that the harvester, in both studies, is very wide (width = 0.6260 of length), which generates a broader natural frequency than a slender one.

Figure 17 shows the mesh accuracy of our COMSOL model. Figure 18 shows the calculated first mode natural frequency using Eigen frequency study (COMSOL) which is 49.5 HZ compared with 48.4 HZ of reference (Kouritem and Altabay 2022) with a 2.2% difference. Figure 19 reveals the mesh accuracy of the two-mass model, where the first mass is 12 g and the second mass is 4 g only. The locations of the two masses are shown in Fig. 19. Also, the two masses model was used to prove that increasing the number of masses increases the broadband natural frequency and the output voltage. The results of the comparison are exposed in Fig. 20. The numerical results of voltage frequency response are in good agreement with experimental results introduced by reference (Kouritem and Altabay 2022). The maximum voltage calculated using FEM was 102.82 V, while the recorded experimentally by reference (Kouritem and Altabay 2022) was 100 V with a 2.82% difference. Moreover, Fig. 20 shows the frequency response of the two masses model compared with the one-mass model. For the two-masses model, the maximum voltage is 146 V at 52.4 Hz (first mode natural frequency), so, the two-masses model produces a larger voltage and wider broadband natural frequency than the one-mass model.

6 Conclusion

Since vibration sources often have the characteristics of broadband frequency, the problem of power drop due to the variation in excitation frequency arises. It was concluded that natural frequency broadening was the solution to increase the effective natural frequency. To enlarge the

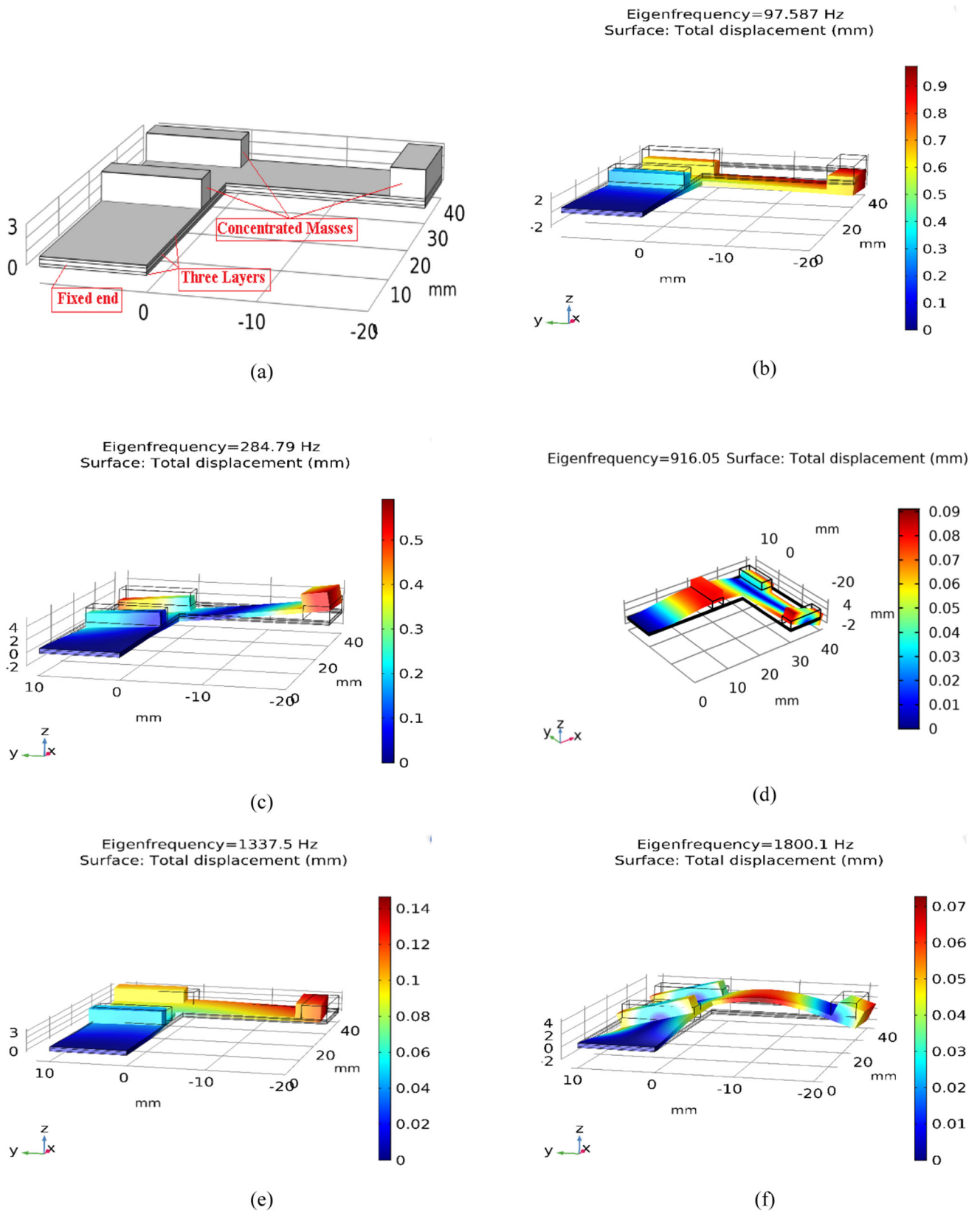


Fig. 10 L-shaped harvester with concentrated masses and its mode. **a** model **b** first mode **c** second mode **d** third mode **e** fourth mode **f** fifth mode

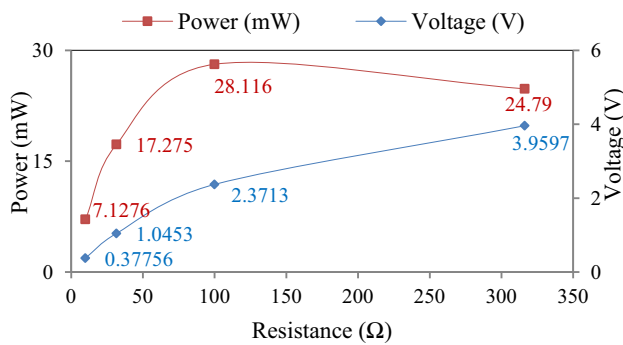


Fig. 11 The resistance dependence of the power and voltage

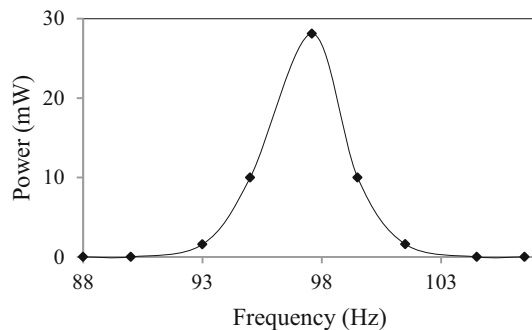


Fig. 12 The output power- frequency relation

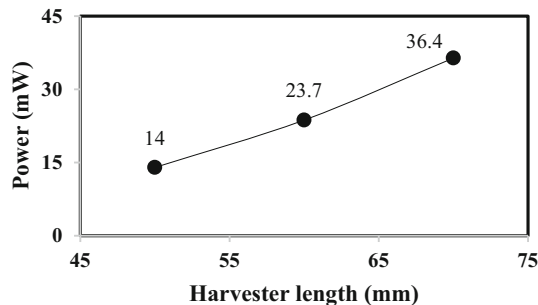


Fig. 13 Effect of harvester length on the output power

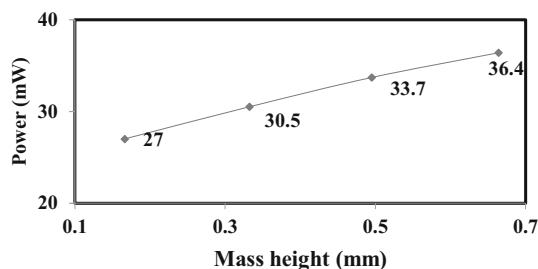


Fig. 14 Effect of mass height on output power

natural frequency band range, the multi-mass single harvester was utilized. Four harvesters were designed, simulated, and compared to grasp the best way of broadening

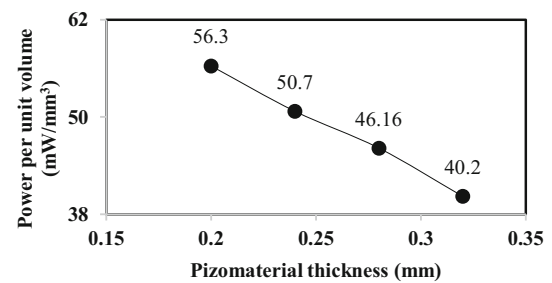


Fig. 15 Effect of piezoelectric thickness on the output power

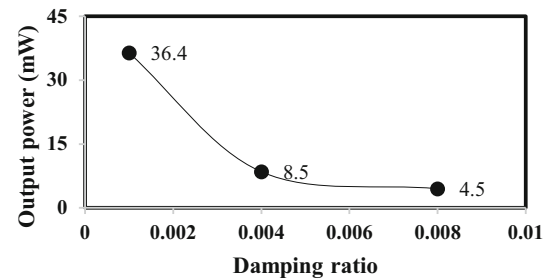


Fig. 16 Effect of damping ratio on the output power

the natural frequency. The summary of the main highlights is listed as follows:

1. The FEM COMSOL is validated with experimental results of the literature and is found to be in good agreement. The wider harvester with (high width/length) gives more wideband natural frequency.
2. The results proved that the increase of the concentrated masses number increases both the broadband natural frequency and the output power.
3. The power per unit volume was about $41.9 \times 10^{-3} \text{ mW/mm}^3$ and $56.3 \times 10^{-3} \text{ mW/mm}^3$ for L-shaped harvester and harvester with concentrated masses, respectively. Thus, the study results prove that the rectangular harvester cantilever with concentrated masses is more effective than the L-shaped one.
4. The increase of the broadband frequency of the six masses harvester and the three masses harvester was about 66 and 51% that of the harvester without added mass, respectively.
5. The increase in beam length and mass height increases the output power while the increase in piezoelectric thickness and damping ratio decreases the output power and bandwidth frequency.
6. Since many vibration sources have a fluctuating excitation frequency, it is recommended to design, analyze, and optimize a harvester array (multiple harvesters) with successive resonant frequencies to target the vibration range.
7. This research results prove that; the bending stress harvester is more effective than the torsion-bending

Table 8 Material and geometric parameters of the harvester utilized for validation (Kouritem and Altaby 2022)

Parameters	Brass	Piezoelectric	Material	Brass	PZT-5A
Length (mm)	50.8	50.8	Density (kg m ⁻³)	9000	7800
Width (mm)	31.8	31.8	Young’s modulus (GPa)	105	66
Thickness (mm)	0.14	0.26	Piezo. constant, d31 (pm V ⁻¹)	–	– 190
Tip first mass (Kg)	0.012		Permittivity (F m ⁻¹)	–	1500
Second mass (Kg)	0.004		Acceleration(m/s ²)	9.81	470e ³

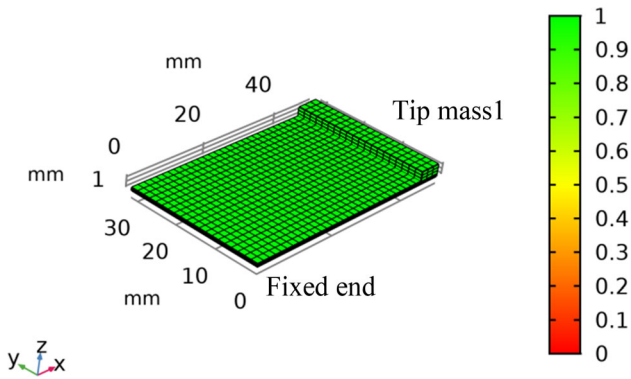


Fig. 17 Mesh accuracy (efficiency) of one mass model

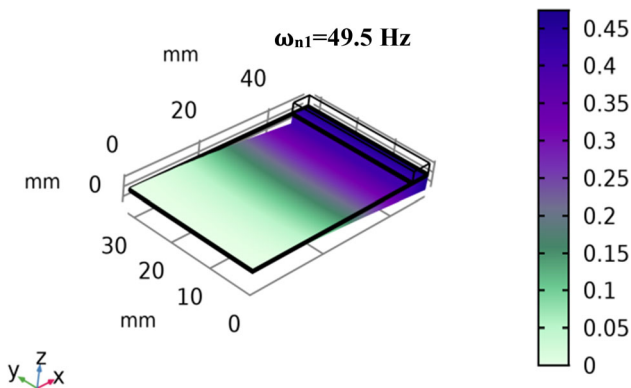


Fig. 18 First mode natural frequency and its displacement

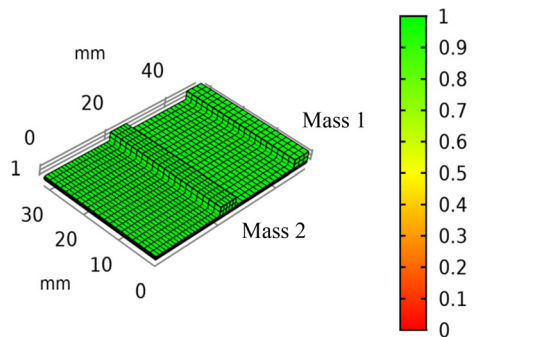


Fig. 19 Mesh accuracy of two masses model

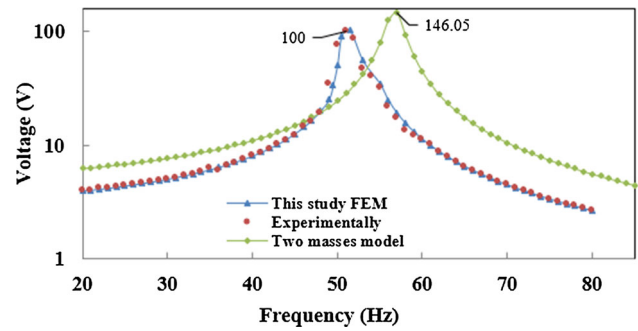


Fig. 20 Frequency–voltage responses of the one mass harvester and two masses of this study of reference (Kouritem and Altaby 2022)

7 Future work

In future work, it is suggested to investigate the effect of two sliding masses on L-shape cantilever on the broadband natural frequency and output power.

Appendix

Table parameters and abbreviations.

Abbreviations

ART	Automatic Resonance Tuning
FEM	Finite Element Method
MEMS	Microelectromechanical Systems
PVDF	Polyvinylidene Fluoride
ART	Automatic Resonance Tuning

Parameters

w_n	Natural frequency
V_{re}	Rectified voltage
c_p	Capacitance
C_V	Damping coefficient
M	Dynamic mass
U	Base excitation
R	Load resistance

harvester in both widening the natural frequency and increasing the output power.

Acknowledgements Authors would like to thank the Smart critical infrastructure research Centre High-performance Computer Lab, Alexandria University, Egypt. The COMSOL 6 was utilized. hardware systems specifications were RAM=128 GB, Processor 2.6 GHz, and Hard=1tera.

Funding Open access funding provided by The Science, Technology & Innovation Funding Authority (STDF) in cooperation with The Egyptian Knowledge Bank (EKB). This work was funded by Alexandria University.

Data availability The data are available on request from the corresponding author.

Declarations

Conflict of interest The authors declare that they have no known competing financial interests or personal relationships that could have appeared to influence the work reported in this paper.

Open Access This article is licensed under a Creative Commons Attribution 4.0 International License, which permits use, sharing, adaptation, distribution and reproduction in any medium or format, as long as you give appropriate credit to the original author(s) and the source, provide a link to the Creative Commons licence, and indicate if changes were made. The images or other third party material in this article are included in the article's Creative Commons licence, unless indicated otherwise in a credit line to the material. If material is not included in the article's Creative Commons licence and your intended use is not permitted by statutory regulation or exceeds the permitted use, you will need to obtain permission directly from the copyright holder. To view a copy of this licence, visit <http://creativecommons.org/licenses/by/4.0/>.

References

- Altabey WA, Kouritem SA (2022) “The new techniques for piezoelectric energy harvesting: design optimization applications and analysis. *Energies* 15:6684
- Andrzej K, Krzysztof W (2016) Modelling and testing of the piezoelectric beam as energy harvesting system. *Acta Mechanica Automatica* 10:291–295
- Bani-Hani M, Almomani A, Aljanaideh K, Kouritem SA (2022) Mechanical modeling and numerical investigation of earthquake-induced structural vibration self powered sensing device. *IEEE Sens J*. <https://doi.org/10.1109/JSEN.2022.3204719>
- Bani-Hani MA, Husein Malkawi DA, K. A. Bani-Hani S. A. Kouritem, (2023) Genetic algorithm optimization of rainfall impact force piezoelectric sensing device analytical and finite element investigation. *Materials* 16:911
- Cao D, Xia W, Hu W (2019) Low-frequency and broadband vibration energy harvester driven by impact based on layer-separated piezoelectric beam”. *Appl Math Mech* 12:1777–1790
- Ceponis A, Mažeika D, Kilikevicius A (2019) Bidirectional piezoelectric energy harvester. *Sensors* 19(1–24):3845
- Chen Z, Yang Y, Lu Z, Luo Y (2013) Broadband characteristics of vibration energy harvesting using one-dimensional phononic piezoelectric cantilever beams”. *J Phys B* 410:5–12
- Elshabasy MMYB, Kouritem SA (2020) Thickening of optimally selected locations on panels subjected to unyawed flow for substantial delay of the panel flutter. *Alex Eng J* 59(6):5031–5044. <https://doi.org/10.1016/j.aej.2020.09.026>
- Erturk A, Inman DJ (2009) “An experimentally validated bimorph cantilever model for piezoelectric energy harvesting from base excitations. *Smart Mater Struct* 18(1–18):025009
- Aktakka E. E. ,Peterson R. L. , and NajafiK. (2011) “Thinned-PZT on SOI process and design optimization for piezoelectric inertial energy harvesting”, 16th International Solid-State Sensors, Actuators and Microsystems Conference, University of Michigan, USA, pp. 1649–1652.
- Ferrari M, Ferrari V, Guizzetti M, Marioli D, Taroni A (2008) Piezoelectric multifrequency energy converter for power harvesting in autonomous microsystems. *Sens Actuator A Phys* 142:329–335. <https://doi.org/10.1016/j.sna.2007.07.004>
- Hong Y, Sui L, Zhang M, Shi G (2018) Theoretical analysis and experimental study of the effect of the neutral plane of a composite piezoelectric cantilever. *Energy Convers Manage* 171:1020–1029
- Hung CF, Chung TK, Yeh PC, Chen CC, Wang CM, Lin SH (2015) A miniature mechanical-piezoelectric configured three-axis vibrational energy harvester. *IEEE Sens J* 15:5601–5615
- Iannacci J (2017) Microsystem based Energy Harvesting (EH-MEMS): powering pervasivity of the internet of things (iot) – a review with focus on mechanical vibrations. *J K Saud Univ Sci* 31:66–74
- Khazaei M, Rezaniakolaie A, Rosendahl L (2020) A broadband macro-fiber-composite piezoelectric energy harvester for higher energy conversion from practical wideband vibrations. *Nano Energy* 76:1–11
- Kim HW, Priya S, Uchino K, Newnham RE (2005) Piezoelectric energy harvesting under high pre-stressed cyclic vibrations. *J Electroceram* 15:27–34
- .Kouritem S.A (2021) Array of piezoelectric energy harvesters for broadband natural frequency applications ICSV27, Annual Congress of International Institute of Acoustics and Vibration (IIAV) Prague, 11–16 July.
- Kouritem SA, Altabey WA (2022) Ultra-broadband natural frequency using automatic resonance tuning of energy harvester and deep learning algorithms. *Energy Convers Manage* 272:116332
- Kouritem SA, Elshabasy MMYB (2021) Tailoring the panel inertial and elastic forces for the flutter and stability characteristics enhancement using copper patches. *Compos Struct* 274:114311. <https://doi.org/10.1016/j.compstruct.2021.114311>
- Kouritem SA, Al-Moghazy MA, Noori M, Altabey WA (2022a) “Mass tuning technique for a broadband piezoelectric energy harvester array. *Mech Syst Signal Proc* 181:109500
- Kouritem SA, Bani-Hani MA, Beshir M, Elshabasy MMYB, Altabey WA (2022b) Automatic resonance tuning technique for an ultra-broadband piezoelectric energy harvester. *Energies* 15:7271. <https://doi.org/10.3390/en15197271>
- Kouritem SA, Abouheaf MI, Nahas N, Hassan M (2022c) A multi-objective optimization design of industrial robot arms. *Alex Eng J* 61:12847–12867
- Lafarge B, Grondel S, Delebarre C, Cattan E (2018) A validated simulation of energy harvesting with piezoelectric cantilever beams on a vehicle suspension using bond Graph approach. *Mechatronics* 53:202–214
- Lefevre DAE, Richard C, Guyomar D (2007) Buck-Boost converter for sensorless power optimization of piezoelectric energy harvester. *Transact Power Electron* 5:20–34
- Lia H, Liub D, Wangb J, Shangb X, Hajje M (2020) Broadband bimorph piezoelectric energy harvesting by exploiting bending-torsion of L-shaped structure. *Energy Convers Manage* 206(1–16):112503
- Lien IC, Shu YC (2012) Array of piezoelectric energy harvesting by the equivalent impedance approach. *Smart Mater Struct* 21:082001

- Liu J-Q, Fang H-B, Xu Z-Y, Mao X-H, Shen X-C, Chen D, Liao H, Cai B-C (2008) A MEMS-based piezoelectric power generator array for vibration energy harvesting. *Microelectron J* 39:802–806. <https://doi.org/10.1016/j.mejo.2007.12.017>
- Liu H, Quan C, Tay CJ, Kobayashi T, Lee C (2011) A MEMS-based piezoelectric cantilever patterned with PZT thin film array for harvesting energy from low frequency vibrations. *Phys Procedia* 19:129–133
- Liu CLH, Kobayashi T, Jui Tay C, Quan C (2012) A new S-shaped MEMS PZT cantilever for energy harvesting from low frequency vibrations below 30 Hz *Microsyst Technol. Microsyst Technol* 18:497–506
- Lumentut MF, Howard IM (2013) Analytical and experimental comparisons of electromechanical vibration response of a piezoelectric bimorph beam for power harvesting. *Mech Syst Signal Process* 36:66–86
- Mehrabi H, Hamed M, Aminzahed I (2020) A novel design and fabrication of a micro-gripper for manipulation of micro-scale parts actuated by a bending piezoelectric. *Microsyst Technol* 26:1563–1571
- Mohamed KT, El-Gamal HA, Kouritem SA (2021) An experimental validation of a new shape optimization technique for piezoelectric harvesting cantilever beams. *Alex Eng J* 60:1751–1766
- Moon K, Choe J, Kim H, Ahn D, Jeong J (2018) A method of broadening the bandwidth by tuning the proof mass in a piezoelectric energy harvesting cantilever. *Sens Actuators, A* 276:17–25
- Nader G, Silva ECN, Adamowski JC (2004) Effective damping value of piezoelectric transducer determined by experimental techniques and numerical analysis. *ABCM Sympos Ser Mechatron.* 1:271–279
- Naqvi A, Ali A, Altabey WA, Kouritem SA (2022) Energy harvesting from fluid flow using piezoelectric materials: a review. *Energies* 15:7424. <https://doi.org/10.3390/en15197424>
- Peigney M, Siegert D (2013) Piezoelectric energy harvesting from trac-induced bridge vibrations. *Smart Mater Struct* 22:095019
- Ramírez JM, Gatti CD, Machado SP, Febbo M (2018) A multi-modal energy harvesting device for low-frequency vibrations. *Extreme Mech Lett* 22:1–7
- Roundy S, Wright PK, Rabaey J (2003) A study of low level vibrations as a power source for wireless sensor nodes. *Comput Commun* 26:1131–1144
- Shaukat H, Ali A, Bibi S, Altabey WA, Noori M, Kouritem SA (2023) A Review of the recent advances in piezoelectric materials, energy harvester structures, and their applications in analytical chemistry. *Appl Sci* 13:1300
- Shin Y, Choi J, Jin Kim S, Kim S, Maurya D, Sung T, Priya S, Kang C, Song H (2020) Automatic resonance tuning mechanism for ultra-wide bandwidth mechanical energy harvesting. *Nano Energy* 77:1–11
- Song J, Zhao G, Li B, Wang J (2017a) Design optimization of PVDF-based piezoelectric energy harvesters. *Heliyon* 3:00377
- Song H-C, Kumar P, Maurya D, Kang M-G, Reynolds WT, Jeong D-Y, Kang C-Y, Priya S (2017b) Ultra-low resonant piezoelectric MEMS energy harvester with high power density. *J Microelectromech Syst* 26:1226–1234
- Song H-C, Kumar P, Sriramdas R, Lee H, Sharpes N, Kang M-G, Maurya D, Sanghadasa M, Kang H-W, Ryu J, Reynolds WT, Priya S (2018) Broadband dual phase energy harvester: vibration and magnetic field. *Appl Energy* 225:1132–1142. <https://doi.org/10.1016/j.apenergy.2018.04.054>
- Williams C. B. and Yates R. B. (1995) “ Analysis of a micro-electric generator for microsystems”, in *Proc. 8th Int. Conf. Solid-State Sensors Actuators, Eurosensors IX Transducers*, Sweden, vol. 1, pp. 369–372.
- Williams CB, Yates RB (1996) Analysis of a micro-electric generator for microsystems. *Sens Actuators, A* 52(1–3):8–11
- Wu X, Lee D (2019) Miniaturized piezoelectric energy harvester for battery-free portable electronics Short Communication. *Int J Energy Res* 20:2402–2409
- Wu J, Chen X, Chu Z, Shi W, Yu Y, Y., S. Dong, (2016) A barbell-shaped high-temperature piezoelectric vibration energy harvester based on BiScO₃-PbTiO₃ ceramic. *Appl Phys Lett* 109:173901
- Yildirim T, Zhang J, Sun S, Alici G, Zhang S, Li W (2017) Design of an enhanced wideband energy harvester using a parametrically excited array. *J Sound Vib* 410:416–428

Publisher's Note Springer Nature remains neutral with regard to jurisdictional claims in published maps and institutional affiliations.